Journal of Alloys and Compounds 500 (2010) 9–15

Contents lists available at ScienceDirect

Journal of Alloys and Compounds

journal homepage: www.elsevier.com/locate/jallcom

Optically induced effects in nano-crystallized $PbO–Sb_2O_3–B_2O_3:Pr_2O_3$ glasses

T. Satyanarayana[a,e], I.V. Kityk[b], Y. Gandhi[a], V. Ravikumar[a], W. Kuznik[c], M. Piasecki[d], M.A. Valente[e], N. Veeraiah[a,*]

[a] Department of Physics, Acharya Nagarjuna University-Nuzvid Campus, Nuzvid 521 201, India
[b] Electrical Engineering Department, Technical University of Czestochowa, Aleja Armii, Krajowej 17/19, PL-42-201 Czestochowa, Poland
[c] Chemical Department, Czestochowa University of Technology, Strzody 9, Gliwice, Poland
[d] Institute of Physics, J. Dluygosz University, Armii Krajowej 13.15, Czestochowa, Poland
[e] Physics Department (13N - FSCOSD), Aveiro University, 3800-193 Aveiro, Portugal

ARTICLE INFO

Article history:
Received 11 March 2010
Accepted 27 March 2010
Available online 3 April 2010

Keywords:
Nonlinear optical effects
Antimony borate glass ceramics
Pr^{3+} ions

ABSTRACT

$PbO–Sb_2O_3–B_2O_3$ glasses mixed with different content of Pr_2O_3 (ranging from 0 to 0.6 mol%) were crystallized. The samples were characterized by X-ray diffraction, transmission electron microscopy (TEM) and differential scanning calorimetric (DSC) techniques. The TEM studies indicated that the samples contain well defined and randomly distributed nanoclusters possessing the sizes within ~30–40 nm. The XRD spectra have exhibited diffraction peaks due to presence of $Pb_5Sb_2O_8$, $Pb_3(SbO_4)_2$, PbB_4O_7, β-$PrSbO_4$, Pr_3SbO_7, $Pr_3Sb_5O_{12}$ crystalline phases. From these spectra, it was identified that the antimony ions co-exist in Sb^{5+} state with Sb^{3+} state in the titled glass ceramic samples. The photo-induced birefringence (changes in refractive indices) caused by simultaneous exposure of the sample with the doubled frequency coherent laser beam (1.54 μm and 0.77 μm) was monitored by polarized probing beam of varying wavelength in the range of 750–1250 nm. The induced birefringence exhibited a maximum at about 1000 nm, a wavelength corresponding to $^3H_4 \rightarrow {}^1G_4$ optical excitation transition of Pr^{3+} ion. We have established a correlation between the intensity of this transition and the birefringence dispersion. Principal role of the photo-occupation of this transition is identified. The variations of photo-induced birefringence with increase in the content of Pr_2O_3 is explained due to the increasing degree of disorder and increasing concentration of deformed PrO_8 structural units in the glass ceramic. Further analysis of these results coupled with the data on IR and Raman spectral studies, has indicated that $PbO–Sb_2O_3–B_2O_3$ glasses crystallized with 0.6 mol% of Pr_2O_3 exhibit maximal birefringence effects.

1. Introduction

The understanding of the origin of optical nonlinearities in glasses and glass ceramics stimulated by ultra-short laser pulses has gained momentum in the recent years; such studies in fact help in examining the suitability of the materials for potential applications like three-dimensional photonic devices for integrated optics and other nonlinear optical devices (such as ultrafast optical switches, power limiters, broad band optical amplifiers) [1,2]. The conventional methods, like ion-exchange, diffusion into a transparent substrate or lithographic methods that are being used for inducing nonlinear optical effects are generally limited to the fabrication of planar or low-dimensional structures. On the other hand, when the ultra-short laser pulses of sufficient intensities are focused into the bulk of glasses and glass ceramic materials, a local redistribution of the electronic charge density takes place; such rearrangement often leads to the modification of the microstructure in the material. Such kind of effects play dominant role in the nonlinear absorption process. Such absorption ultimately induces changes of the refractive index in the material due to multi-photon processes. The degree of the photo-induced nonlinearity depends from one side on the wavelength of the laser pulse, pulse energy, pulse duration, repetition rate and exposure time and from the other side the local structure of the glasses, their crystallization behavior, color center and exciton formation also play a major role in the mentioned effects. The strength and nature of the generated optical nonlinearity can be described in terms of the nonlinear susceptibility of the first and higher orders or equivalently in terms of the changes in the absorption coefficient (amplitude response) and the refractive index (phase response) of the medium.

In case of oxide glasses (which do not possess the inversion symmetry) the optical poling is caused by the formation of a spatially periodic optically induced electrostatic field in the sample due to photo-carrier charge separation by means of direct current due to a coherent photo-galvanic effect [3,4]. In this type of optical poling, there is a spatial periodicity of the photo-induced electric field with a period of q^{-1} ($q = 2k_1 - k_2$, where k_1, k_2 are the wave vectors of fundamental and doubled frequency coher-

* Corresponding author.
E-mail address: nvr8@rediffmail.com (N. Veeraiah).

0925-8388/$ – see front matter © 2010 Elsevier B.V. All rights reserved.
doi:10.1016/j.jallcom.2010.03.221

ent beams). Hence, the periodic space modulation of the refractive index $\Delta n_{ji} \sim \chi^{(3)}_{ijk\ell} E_{0k} E_{0\ell}$ with a period of $(2q)^{-1}$ and the second-order polarizability $\chi^{(2)}_{jkl} = \chi^{(3)}_{ijkl} E_{0\ell}$ with the period of q^{-1} appear in the optical poling. The study of the dispersion of the induced optical susceptibilities (both linear and nonlinear one) thus consists of probing the laser-induced changes in the refractive index of the material as a function of the varying probe wavelength.

So far, most of the studies on optically stimulated nonlinear optical effects are limited to silicate glasses because of their wide use as optical materials. The antimony oxide based glass ceramics can be considered as equally better candidates for inducing NLO effects since these materials possess high refractive index, they have relatively large polarizability and are transparent to the far infrared wavelengths [5,6]. Sb_2O_3 participates in the glass network with SbO_3 structural units and can be viewed as tetrahedrons with the oxygen situated at three corners and the lone pair of electrons of antimony (Sb^{3+}) at the fourth corner localized in the third equatorial direction of Sb atom. The charge density deformability of this pair probably could make these glass ceramics to exhibit first order nonlinear optical susceptibility described by third rank polar tensors due to occurrence of photo-induced non-centrosymmetry. However, Sb_2O_3 is an incipient glass network former and as such does not readily form the glass; hence to facilitate the glass formation, mixing of some proportion of a strong glass former like B_2O_3 is necessary. Moreover, following the relatively high values of local polarizabilities, one can expect that glasses containing borate may also be of particular interest for the photo-induced nonlinear optics [7].

The addition of PbO to Sb_2O_3–B_2O_3 mixture further assists the formation of a good glass since it acts not only as a modifier but also as a glass former participating in the glass network with [$PbO_{4/2}$] pyramidal units connected in puckered layers. Additionally, earlier it was also reported that PbO also plays a crucial role in inducing the nonlinear optical effects in the glass materials [8].

Kityk et al. have demonstrated that partial crystallization of the glass-like materials leads to substantial enhancement of the photo-induced SHG [9]. Recently, we have reported the second-order nonlinear optical effects of antimony borate glasses crystallized with TiO_2 and CoO as nucleating agents [10]. From these studies, the optimal concentrations of the dopant ions/crystallizing agents for getting the maximum optically induced effects have been identified.

Additional possibilities are opened by use of rare earth doped nano-crystalline glass materials. Some recent studies on PIB effects of rare earth mixed crystalline materials are available in the literature [7]. The crystallization of especially antimony oxide based glasses is of more interesting since during the crystallization, there exists a possibility for oxidation of a part of Sb^{3+} ions and transforming it to Sb^{5+} state. These Sb^{5+} ions participate in the glass network forming with $Sb^{5+}O_4$ structural units and likely to link with BO_4 structural units in PbO–Sb_2O_3–B_2O_3 glass ceramic network [11]. There are also reports suggesting that the Sb^{5+} ions especially in the glasses mixed with rare earth ions form the crystals of the type Ln_3SbO_7 in which these ions occupy octahedral sites [12]. The local structure of Sb^{5+} ions that participate in the glass network with SbO_6 structural units is expected to be more asymmetric (it is the same as local charge density non-centrosymmetry determining the first order nonlinear optical susceptibilities). The strain energy in the glass network increases as a whole, thus resulting in a decrease in the additional activation energy that is necessary for glass network rearrangement. As a consequence, we expect more degree of disorder in glass ceramics containing more $Sb^{v}O_6$ structural units. Such disorders (in addition to the photo-induced deformability of lone pair of electrons) in the local structure may lead to enhancement in the optically stimulated liner and nonlinear optical coefficients manifesting in the measured changes of the refractive indices.

Praseodymium mixed glasses are being widely investigated, in view of the fact that these glasses exhibit very rich emission extending from UV to infrared region. Pr-mixed glass fibers are currently being used as the most promising candidates for a 1.3 μm ($^1G_4 \rightarrow {}^3H_5$) communication window. It may be worth mentioning here that the world land-based optical networks are composed of 1.3 μm (O-band) zero-dispersion silica fiber, much attention are paid to the $^1G_4 \rightarrow {}^3H_5$ transition of Pr^{3+} in developing 1.3 μm all-optical signal amplifiers [13–15].

In view of these facts, it is felt worth to investigate the optically stimulated effects in Pr^{3+} ions mixed PbO–Sb_2O_3–B_2O_3 glass ceramics containing nano-sized crystals. The main objective of the present investigation is to study the influence of crystallization to nano-level on the photo-induced changes (variations in the refractive index with the probe wavelength) of Pr^{3+} ions mixed lead antimony borate glass system. The results of the auxiliary experiments viz., IR, Raman and optical absorption, that help for the analysis of photo-induced optical effects have also been reported.

2. Experimental methods

From the glass-forming region of PbO–Sb_2O_3–B_2O_3 glass system [10], the following composition is chosen for the present study: $(30-x)$PbO–40Sb_2O_3–30B_2O_3:xPr_2O_3 with x = 0.2 (P_2), 0.4 (P_4) and 0.6 (P_6); the corresponding post-heated samples are labeled as CP_2, CP_4 and CP_6 respectively. The details of methods adopted for the preparation of the glass samples were reported in our earlier papers [10]. The glass specimens with various concentrations of Pr_2O_3 were heat treated in a furnace at (a temperature corresponding to crystallization peak temperature identified from DSC studies) 570–580 °C for 24 h. Automatic controlling furnace was used to keep the temperature at the desired level. After the heat treatment in the furnace at fixed temperature, the samples were chilled in air to room temperature. The samples prepared were ground and optical polished to the dimensions of 1 cm × 1 cm × 0.2 cm. The crystalline phases in the glass ceramic samples were identified by recording XRD spectra using Rigaku D/Max ULTIMA III X-ray diffractometer with Cu Kα radiation with angle resolution of 0.02°. Transmission electron microscopy studies were carried out on these samples to observe the crystallinity using JEOL-100C transmission electron microscope (TEM) with the 100 kV electron beam. These observations were performed in a bright field regime with an objective aperture of size 9 nm^{-1} in a back focal plane. It is observed that during the performance of these experiments, there is almost no damage taken place to the studied glass ceramic samples. The refractive index (n) of the samples at λ = 589.3 nm was measured to an accuracy of ±0.001 at room temperature using Abbe refractometer with monobromonaphthalene as the contact layer between the glass and the refractometer prism. Thermal analysis was carried out by Netzsch Simultaneous DSC/TG Thermal Analyzer STA409C with 32-bit controller to determine the glass transition temperature and crystalline peaks. High temperature furnace together with a sample carrier and Al_2O_3 crucibles were used. Apparatus was calibrated both for temperature and for sensitivity with melting temperatures and melting enthalpies of the pure metals: Ga, In, Sn, Zn, Al, Ag, Au. All the recordings were carried out in argon (5N) atmosphere to prevent samples from oxidation. Heating rate was 10 °C/min in the temperature range of 32–1300 °C. The density of the glass ceramics was determined to an accuracy of (±0.0001) by the standard principle of Archimedes' using o-xylene (99.99% pure) as the buoyant liquid. The optical absorption spectra of the samples were recorded at room temperature in the spectral wavelength range covering 300–2200 nm with a spectral resolution of 0.1 nm using JASCO Model V-670 UV–vis–NIR spectrophotometer. Infrared transmission spectra were recorded on a JASCO-FT/IR-5300 spectrophotometer upto a resolution of 0.1 cm^{-1} in the spectral range of 400–2000 cm^{-1} using potassium bromide pellets (300 mg) containing pulverized sample (1.5 mg). These pellets were pressed in a vacuum die at ~680 MPa. The Raman spectra were recorded with an NIR excitation line (1064 nm) using a Bio-Rad spectrometer FTS 175C equipped with an FT Raman supplementary accessory working in a back-scattering geometry system.

The study of the dispersion of the induced nonlinearity of the samples was carried out with the bicolor optical treatment with simultaneous registration of the Δn (Fig. 1). The experimental setup for the measurement of induced changes in the refractive index Δn is shown in Fig. 1. A probe beam of varying wavelength (emitted from tungsten-halogen lamp fitted to spectrophotometer Specord 80M) is allowed to incident upon the sample after polarization by a polarizer P. The fundamental frequency radiation of pulsed Er-glass laser with ~1.54 μm (duration of the laser pulses 10 ns, pulse energy up to 1.4 GW/cm^2, repetition frequency 100 Hz) is simultaneously made to impinge (along with the doubled frequency beam obtained by allowing the fundamental beam to pass through KTP crystal with appropriate orientation) upon the sample. The effective phase retardation due to optically induced

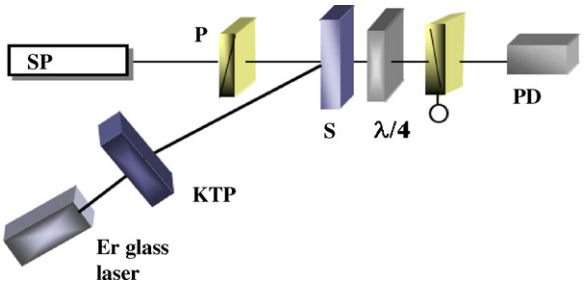

Fig. 1. The experimental setup for the measurement of induced changes in the refractive index (Δn).

effect of the out coming beam is changed by the quarter wave-plate and the analyzer with nonius regite the angle corresponding to the minimum light transmission by the photo-detector D. The setup allows measuring the birefringence with precision up to 10^{-5}. The saturation of the birefringence was achieved after 3–5 min of treatment by bicolor coherent laser Er-glass light. It may be noted here that no macroscopic crack formation could be visualized in these samples after this treatment. The wavelength of the probe beam was varied from 750 to 1250 nm.

3. Results and discussion

The TEM pictures of a pre-heated sample (P_2) and two of the crystallized samples (CP_4 and CP_6) are shown in Fig. 2. The pictures of post-heated samples have exhibited well defined, randomly distributed clusters of crystals (of the size 30–40 nm) ingrained in glassy matrix. The residual glass phase is acting as interconnecting zones among the crystallized areas making the samples free of voids and cracks. Thus, these pictures have clearly confirmed that the samples were converted into glass ceramics after the heat treatment. For further confirmation of the crystalline nature of the samples and for the identification of various crystalline phases, we have also recorded XRD spectra for these samples. X-ray diffraction patterns clearly exhibited micro-structural changes. $Pb_5Sb_2O_8$, $Pb_3(SbO_4)_2$, PbB_4O_7, β-$PrSbO_4$, Pr_3SbO_7, $Pr_3Sb_5O_{12}$ that are kinetically and thermodynamically feasible seemed to be the main products in these samples. The diffraction spectrum for one of the samples (viz., CP_6) is shown in Fig. 3 along with the standard profiles for the crystalline phase Pr_3SbO_7. The presence of peaks due to Pr_3SbO_7, $Pr_3Sb_5O_{12}$ crystalline phases, clearly suggests that antimony ions co-exist in Sb^{5+} state along with Sb^{3+} state in these samples.

Fig. 4 shows differential scanning calorimetric (DSC) scans for $PbO–Sb_2O_3–B_2O_3$ glass and glass ceramic containing 0.6 mol% of Pr_2O_3. DSC trace of glass P_6 exhibited typical glass transition

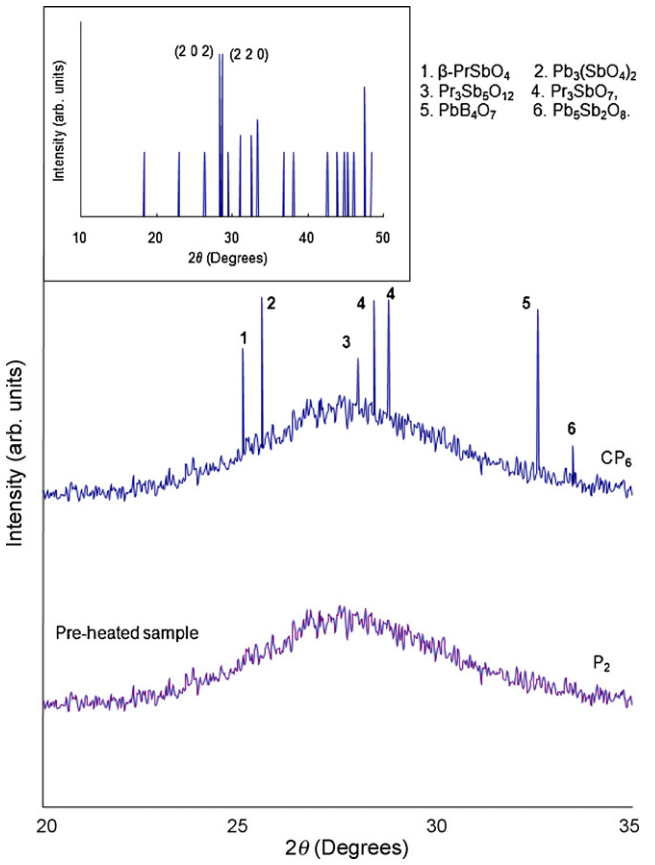

Fig. 3. XRD patterns of $PbO–Sb_2O_3–B_2O_3$ glasses crystallized with 0.2 mol% of Pr_2O_3. Inset represents the standard XRD profile of Pr_3SbO_7 crystalline phase.

temperature at 291 °C followed by an exothermic effect due to crystallization. The DSC thermogram of crystallized sample (CP_6) exhibited an exothermic effect due to glass transition temperature followed by well-defined broad exothermic effects at multiple steps of crystallization temperatures. The multiple crystallization peaks exhibited by this thermogram suggests that the samples under study contain different crystalline phases. The analysis of the results of the DSC studies of the other samples has revealed the similar conclusions.

The infrared transmission spectrum of glass ceramic sample P_2 (Fig. 5) exhibited three conventional bands originated from borate

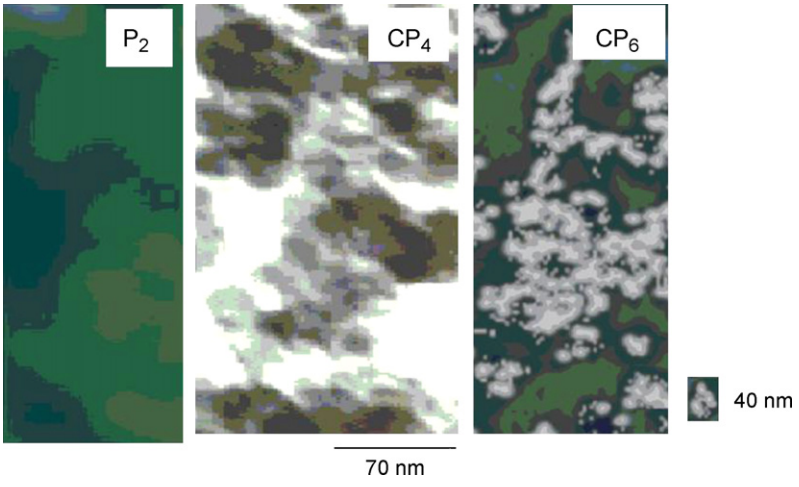

Fig. 2. TEM pictures of some of $PbO–Sb_2O_3–B_2O_3$:Pr_2O_3 glass and glass ceramic samples.

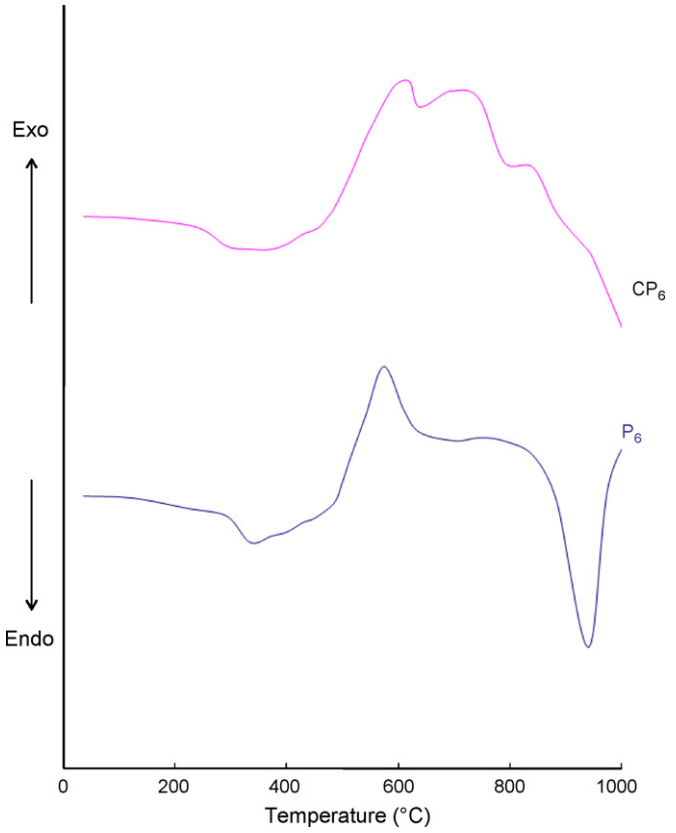

Fig. 4. DSC traces of PbO–Sb_2O_3–B_2O_3 glass and glass ceramic doped with 0.6 mol% of Pr_2O_3.

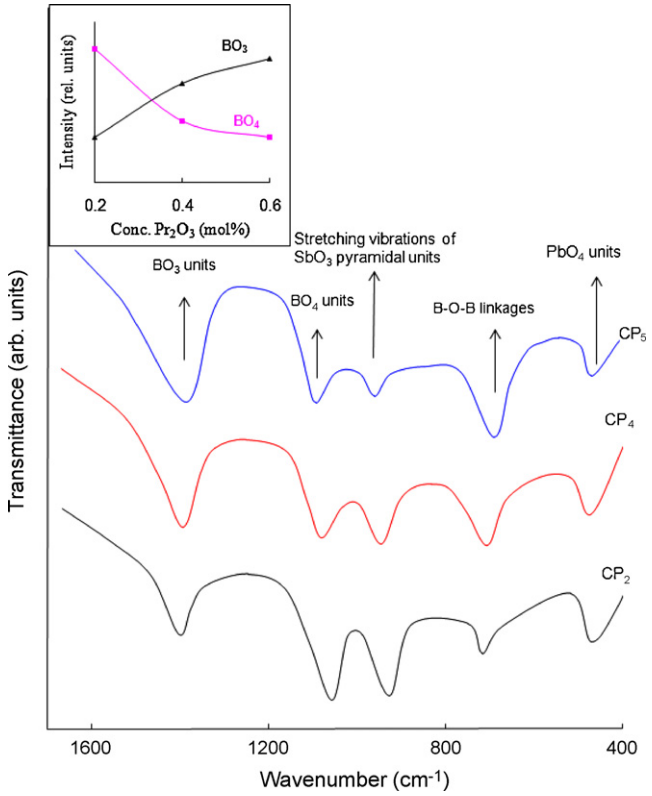

Fig. 5. IR spectra of PbO–Sb_2O_3–B_2O_3:Pr_2O_3 glass ceramics.

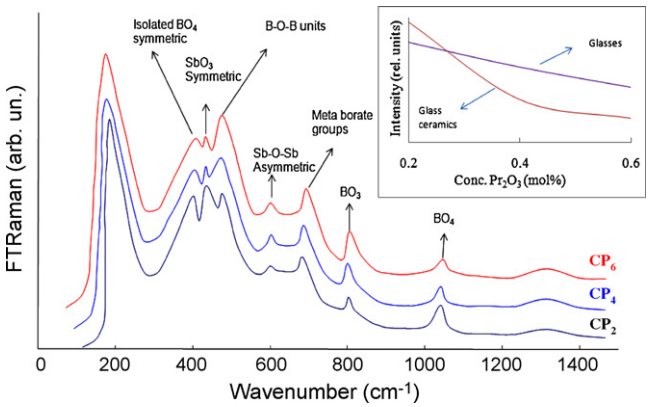

Fig. 6. FT Raman spectra of PbO–Sb_2O_3–B_2O_3:Pr_2O_3 glass ceramics. Inset represents the comparison plot of variation of intensity of the peak due to BO_4 units with the concentration of Pr_2O_3 for glasses and glass ceramic samples.

groups at 1403 cm^{-1} (due to BO_3 units), 1057 cm^{-1} (due to BO_4 units) and another band at 718 cm^{-1} due to bending vibrations of B–O–B linkages [16]. In the spectrum of this sample, the ν_1 vibrational band of SbO_3 units is appeared at 929 cm^{-1} whereas the ν_2 and ν_4 vibrational bands of these units seem to be missing. The ν_3 vibrational band appears to be merged with the band due to bending vibrations of B–O–B linkages and may have formed a common vibrational band due to B–O–Sb linkages. In addition, a band due to PbO_4 structural groups at about 471 cm^{-1}, is also observed in the spectra of all the samples [17]. With the gradual increase in the concentration of crystallizing agent Pr_2O_3, the intensity of bands due to BO_3 and SbO_3 structural units is observed to increase (with a shift of meta center towards lower wavenumber) where as that of the bands due to BO_4 structural units is observed to decrease. A comparison of intensity of the bands due to BO_3 and BO_4 structural units of the pre-heated and post-heated samples is shown as the inset of Fig. 5. The figure clearly suggests that there is a gradual increase in the intensity of the band due to BO_3 units at the expense of more structurally ordered BO_4 units; this observation indicates that there is a higher degree of disorder in the samples crystallized with higher concentrations of Pr_2O_3.

The Raman spectra (Fig. 6) of sample CP_2 exhibited bands at about 684 cm^{-1}, 802 cm^{-1} and 1039 cm^{-1}; these bands attributed to vibrations of chain type meta borate groups, boroxyl ring oxygen breathing of BO_3 units and diborate groups consisting of six membered rings containing two BO_4 tetrahedra, respectively [18]. At about 410 cm^{-1}, a band due to symmetric stretching vibrations of SbO_3 pyramids and another band due to isolated BO_4 structural units at about 400 cm^{-1} are observed [19]. Another broad band spreading over the region of 1300–1400 cm^{-1} is also observed in these spectra; in this broad band region bands due to the vibrational modes of $BØ_2O^-$ triangle linked to $BØ_4$ unit B–O^- in $BØ_2O^-$ triangle and stretching modes in $BØ_3$ triangles (here Ø is the oxygen atom bridging to two boron atoms) are expected [20–22]. Most interestingly, the spectra also exhibited an intense vibrational band at about 174 cm^{-1} due to fourfold coordinated Pb^{2+} ion situated at the apex of the PbO_4 pyramid [23]. As the concentration of the Pr_2O_3 is increased, a gradual decay of intensity of band due to BO_4 structural units is observed. The decay is found to be at much faster rate for the crystallized samples when compared with that of pre-crystallized samples (inset of Fig. 6). Thus the analysis of the results of Raman spectra unambiguously suggests that there is an increasing degree of disorder with increase in the concentration of Pr_2O_3 in the glass ceramic samples leading to the decreasing of the long-range ordering.

The optical absorption spectra of Pr^{3+} mixed PbO–Sb_2O_3–B_2O_3 glasses and glass ceramics recorded at room temperature in the

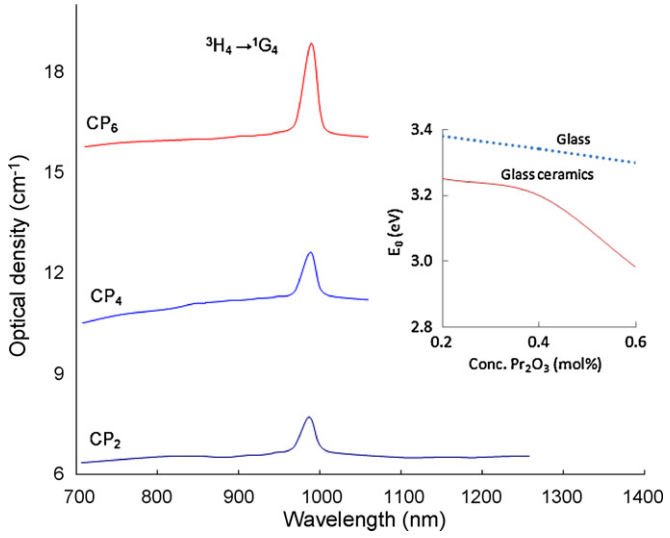

Fig. 7. Optical absorption spectra of $PbO–Sb_2O_3–B_2O_3:Pr_2O_3$ glass ceramics. Inset represents the variation of evaluated optical band gap with the concentration of Pr_2O_3 for the glass and glass ceramic samples.

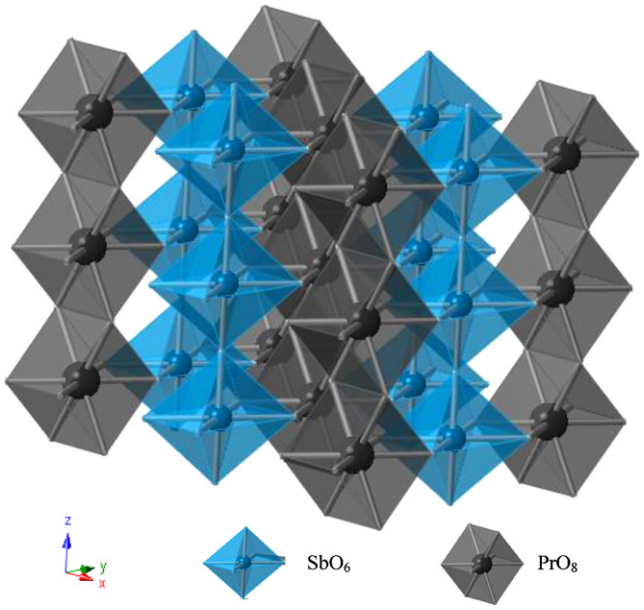

Fig. 8. An illustration of structural fragment of Pr_3SbO_7 crystalline phase.

spectral wavelength range 300–2100 nm, have exhibited several principal absorption bands spread over UV to IR regions. The transitions observed in the spectrum of the sample CP_6 are given below:

$^3H_4 \rightarrow {}^3P_2$(444 nm), $^3P_1$(469 nm), $^3P_0$(483 nm), $^1D_2$(591 nm), $^3F_4$(1426 nm), $^1G_4$(1000 nm), $^3F_3$(1518 nm), $^3F_2$ and $^3H_6$(1910 nm).

However, in the present context, we have concerned the range of 750–1250 nm, in which the photo-induced birefringence is measured. In this region, only one weak absorption band due to $^3H_4 \rightarrow {}^1G_4$ transition is located (Fig. 7). It appears from the figure, the intensity of this band is observed to grow considerably with increase in the content of Pr_2O_3 in the glass ceramics. The absorption under this band is always found to be higher than that of corresponding pre-crystallized samples. Further, in a number of earlier investigations, it was reported that the spectral position of the band due to $^3H_4 \rightarrow {}^3P_0$ transition gives some information regarding the coordination of Pr^{3+} ions in the glass network. To be more precise, the spectral position of this band in the spectral region 20,000–21,000 cm^{-1} suggests coordination number 8 for Pr^{3+} ions in the glass host [24–26]. In the spectra of the present glass ceramics, this particular band (not shown in the figure) observed in the spectral range 20,660–20,750 cm^{-1} allows speculating that Pr^{3+} ions are interlocked in the eight coordination with oxygen atoms in the glass ceramic network. These distorted PrO_8 structural units form a one-dimensional chain through edge-sharing in the glass network. The X-ray diffraction studies as mentioned earlier have indicated that there is a formation of Pr_3SbO_7 crystallites (orthorhombic in shape with unit cell dimensions $a = 10.9442$ Å, $b = 7.5589$ Å, $c = 7.6639$ Å [27]). In such type of crystal phases, Sb^{5+} ions occupy octahedral positions and participate in the glass network with SbO_6 structural units. The Pr_3SbO_7 crystallites consist of the chains of SbO_6 and deformed PrO_8 structural units in alternate parallel planes [12,28]. Based on these arguments, an illustration of structural fragmentation of Pr_3SbO_7 crystalline phase is shown in Fig. 8.

The inset of the Fig. 7 represents the variation of optical band gap, E_0 (evaluated from Urbach plots) with the concentration of Pr_2O_3 for both glass and glass ceramic samples. The plot clearly indicates the lower values of optical band gap for the crystallized samples with respect to the corresponding pre-crystallized samples. The higher concentration of distorted PrO_8 structural units, higher is the concentration of induced non-bridging oxygens (NBOs) in the glass ceramic network. This leads to an increase in the degree of localization of electrons there by increasing the donor centres in the glass ceramic matrix. The presence of larger concentration of these donor centers decreases the optical band gap and shifts the absorption edge towards higher wavelength side as observed. More specifically, the red-shift of E_0 with the increase in the content of Pr_2O_3 in the glass ceramic is associated with increase in the exchange interactions between the p electrons in the conduction band of antimony and the localized 6 s electrons of neighboring Pr^{3+} ions situated in eight coordination with the oxygen ions.

Figs. 9(a and b) give photo-induced birefringence (Δn) with the probe wavelength for the glasses and glass ceramics (mixed with different concentrations of Pr_2O_3) respectively, with simultaneous treatment by polarized bicolor irradiation of the Er-glass laser at 1.54 μm and its second harmonic generation 0.77 μm. It is observed that the value of induced Δn is decreased with increase in probe wavelength with exhibiting a maximum at about 1040 nm for glass and glass ceramic samples containing any concentration of Pr_2O_3. The comparison of induced Δn indicates higher value for the glass ceramics (mixed with any concentration of Pr_2O_3) than that of glasses at any particular probe wavelength. The evaluation of optical band gap indicates lower values for glass ceramics than for the glass samples as mentioned above. The refractive index measured to an accuracy of ±0.001 at room temperature (at the wavelength of 589.3 nm) is varied from 1.592 (CP_2) to 1.598 (CP_6) where as for the glasses it is varied from 1.589 to 1.594. The low optical band gap and high refractive index observed for glass ceramic samples can be considered as responsible for higher photo-induced birefringence in these samples when compared with that of amorphous samples.

For the sake of understanding, in Fig. 10, we have plotted combined variation of Δn and the optical absorption spectra recorded in the same wavelength region for the sample CP_6. The figure clearly confirms that there is a correlation between $^3H_4 \rightarrow {}^1G_4$ transition of Pr^{3+} ion and the maximum of Δn. This observation suggests that diffraction due to induced grating can be attributed to changes in the absorptive part (imaginary part) of the refractive index.

The relation between measured value of absorption coefficient $\Delta\alpha$ at the peak in the absorption spectrum and the changes in the

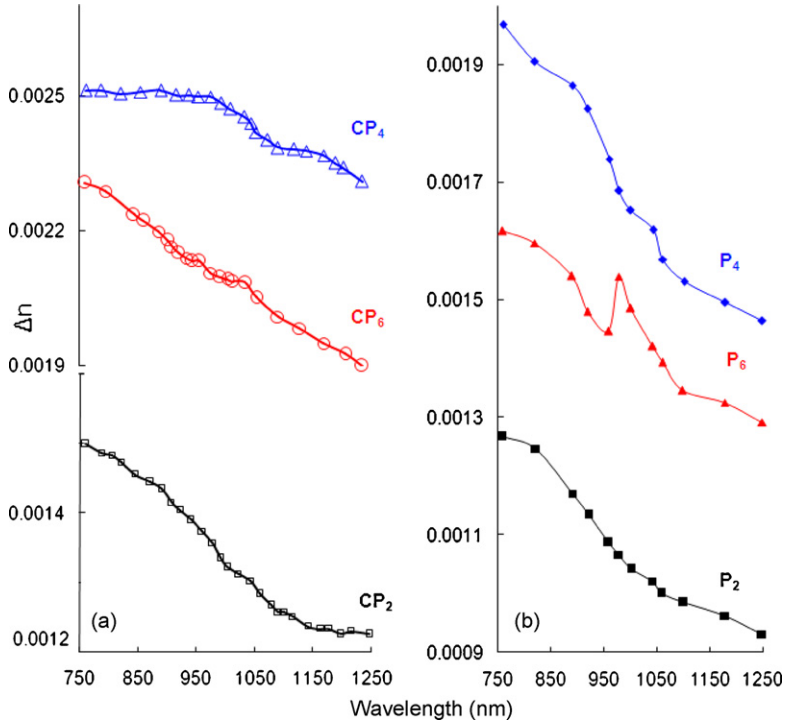

Fig. 9. Photo-induced changes for $PbO–Sb_2O_3–B_2O_3:Pr_2O_3$ (a) glass ceramics and (b) glasses.

real part of the refractive index $\Delta n'(\omega)$ (determined using a weak probe beam of variable frequency ω in the presence of a strong pump at the appropriate frequency) is represented by the conventional Kramers–Kronig (KK) relation as

$$\Delta n'(\omega, I) = \frac{C}{\pi} P \int_0^{\infty} \frac{\Delta\alpha(\omega', I)}{\omega'^2 - \omega^2} d\omega' \quad (1)$$

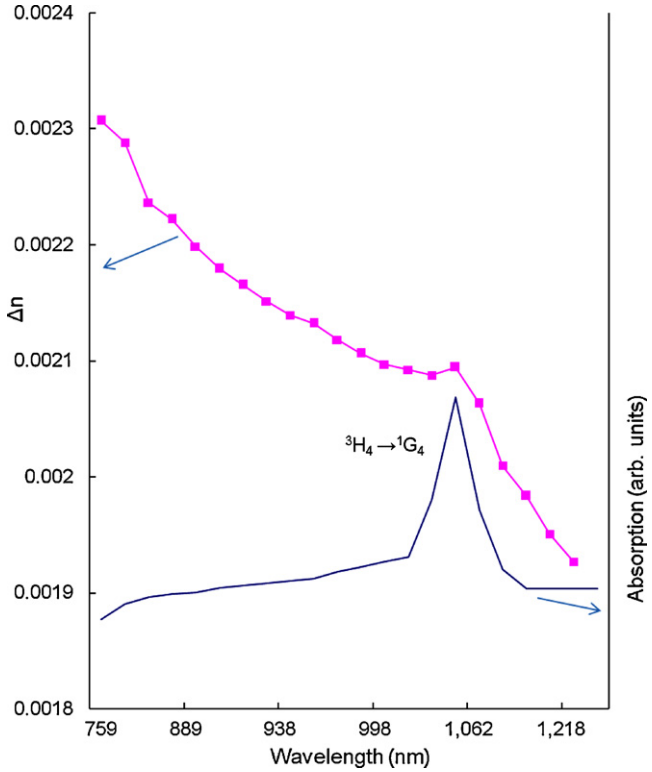

Fig. 10. Comparison of the optical absorption spectrum and photo-induced birefringence for the glass ceramic CP_6.

Here, P refers to Cauchy's principal value and C is the velocity of light and $\Delta\alpha = (1/LN_i)\log(I_0/I)$ with N_i being the rare earth ion concentration (in mol%), L the optical path length (thickness) in cm and $\log(I_0/I)$ the optical density at the peak position. The peaking of Δn at ~1040 nm in the presence of a pump, as per Eq. (1), can therefore be attributed to the building up of maximum population by the pump at $^1G_4$ level. The fall of absorption observed above this wavelength is a result of saturation.

It is necessary to emphasize that the investigated glasses possess substantial advantage with respect to the organic materials [29] which were used for the photo-induced changes due to the higher photo-thermal stability.

4. Conclusions

$PbO–Sb_2O_3–B_2O_3$ glasses have been crystallized to nano-size with different concentrations of Pr_2O_3. The TEM studies indicated that the samples contain well defined and randomly distributed clusters of nanocrystal of the size ~30–40 nm. The XRD studies have pointed out the formation of Pr_3SbO_7 crystalline phase in addition to Sb^{3+} crystal phases. The IR and Raman spectral studies revealed that there is an increasing degree of disorder with increase in the content of Pr_2O_3 in the glass ceramic. The photo-induced changes in the refractive index versus the probe wavelength have exhibited a maximum at the wavelength corresponding to the excitation of $^3H_4 \rightarrow {}^1G_4$ transition of Pr^{3+} ion. The correlation between the two maxima is comprehended due to the maximum photo-excited population by the pump at $^1G_4$ level. The increased photo-induced birefringence with increase in the content of Pr_2O_3 is explained due to the increasing degree of disorder and increasing concentration of deformed PrO_8 structural units in the glass ceramic.

Acknowledgement

One of the authors N. Veeraiah wish to thank Defence Research Development Organization (DRDO), Govt. of India for the financial support of this work.

References

[1] D. Ehrt, T. Kittel, M. Will, S. Nolte, A. Tunnermann, J. Non-Cryst. Solids 345/346 (2004) 332.
[2] K. Divakara Rao, K.K. Sharma, Opt. Commun. 119 (1995) 132.
[3] B.P. Antonyuk, N.N. Novikova, N.V. Didenko, O.A. Aktsipetrov, Phys. Lett. 287 (2001) 161.
[4] M.K. Balakirev, I.V. Kityk, V.A. Smirnov, L.I. Vostrikova, J. Ebothe, Phys. Rev. A 67 (2003) 023806.
[5] K. Terashima, T. Hashimoto, T. Uchino, S. Kim, T. Yoko, J. Ceram. Soc. Jpn. 104 (1996) 1008.
[6] B.V. Raghavaiah, C. Laxmikanth, N. Veeraiah, Opt. Commun. 235 (2004) 341.
[7] A. Majchrowski, J. Ebothe, E. Gondek, K. Ozga, I.V. Kityk, A.H. Reshak, T. Łukasiewicz, J. Alloys Compd. 485 (2009) 29.
[8] E.M. Dianov, P.G. Kazansky, D.S. Starodubov, D.Y. Stepanov, E.R.M. Taylor, Proc. SPIE 2044 (1993) 27.
[9] I.V. Kityk, W. Imiolek, A. Majchrowski, E. Michalski, Opt. Commun. 219 (2003) 421.
[10] T. Satyanarayana, I.V. Kityk, M. Piasecki, P. Bragiel, M.G. Brik, Y. Gandhi, N. Veeraiah, J. Phys.: Condens. Mat. 21 (2009) 245104;
I.V. Satyanarayana, K. Kityk, M. Ozga, P. Piasecki, M.G. Bragiel, V. Brik, A.H. Ravi Kumar, N. Reshak, Veeraiah, J. Alloys Compd. 482 (2009) 283.
[11] D. Holland, A.C. Hannon, M.E. Smith, C.E. Johnson, M.F. Thomas, A.M. Beesley, Solid State NMR 26 (2004) 172.
[12] Y. Hinatsu, H. Ebisawa, Y. Doi, J. Solid State Chem. 182 (2009) 1694.
[13] R. Lobbett, R. Wyatt, P. Eardley, T.J. Whitley, P. Smyth, D. Szebesta, S.F. Carter, S.T. Davey, C.A. Millar, M.C. Brierley, Electron. Lett. 27 (1991) 1472.
[14] K. Wei, D.P. Machewirth, J. Wenzel, E. Snitzer, G.H. Sigel Jr., J. Non-Cryst. Solids 182 (1995) 257.
[15] A. Majchrowski, I.V. Kityk, J. Ebothe, T. Lukasiewicz, J. Appl. Phys. 100 (2006) 053101.
[16] K.J. Rao, Structural Chemistry of Glasses, Elsevier, Amsterdam, 2002.
[17] G. Srinivasarao, N. Veeraiah, J. Solid State Chem. 166 (2002) 104.
[18] D. Maniu, T. Iliescu, I. Ardelean, I. Bratu, C. Dem, Studia Universitatis Babes-Bolyai - Phys. (Special Issue) (2001) 366.
[19] I.R. Beattie, K.M.S. Livingston, G.A. Ozin, D.J. Reynolds, J. Chem. Soc. A (1970) 449.
[20] K. Kotkova, H. Ticha, L. Tichy, J. Raman Spectrosc. 39 (2008) 1219.
[21] M. Srinivasa Reddy, S.V.G.V.A. Prasad, N. Veeraiah, Phys. Status Solidi (a) 204 (2007) 816.
[22] G.D. Chryssikos, M.S. Bitsis, J.A. Kapoutsis, E.I. Kamitsos, J. Non-Cryst. Solids 217 (1997) 278.
[23] A.M. Zahra, C.Y. Zahra, B. Piriou, J. Non-Cryst. Solids 155 (1993) 45.
[24] P. Nachimuthu, R. Jagannathan, Phys. Chem. Glasses 36 (1995) 194.
[25] Q. Su, Y. Lu, Rare Earths Spectroscopy, World Science, Singapore, 1985.
[26] V. Ravikumar, N. Veeraiah, B. Appa Rao, J. Lumin. 75 (1997) 57.
[27] J.F. Vente, R.B. Helmholdt, D.J. Ijdo, J. Solid State Chem. 108 (1994) 18.
[28] T. Fennell, S.T. Bramwell, M.A. Green, Can. J. Phys. 79 (2001) 1415.
[29] G. Lemercier, C. Andraud, I.V. Kityk, J. Ebothe, B. Robertson, Chem. Phys. Lett. 400 (2004) 19.